Reactions of the dichloroboryl complex of osmium, Os(BCl$_2$)Cl(CO)(PPh$_3$)$_2$, with water, alcohols, and amines Crystal structures of Os[B(OH)$_2$]Cl(CO)(PPh$_3$)$_2$, Os[B(OEt)$_2$]-Cl(CO)(PPh$_3$)$_2$, and Os[BN(CH$_3$)C$_6$H$_4$N(CH$_3$)]Cl(CO)(PPh$_3$)$_2$

George R. Clark, Geoffrey J. Irvine, Warren R. Roper *, L. James Wright *

Department of Chemistry, The University of Auckland, Private Bag 92019 Auckland, New Zealand

Dedicated to Professor Fred Hawthorne on the occasion of his 75th birthday and in recognition of his many major contributions to inorganic and boron chemistry

Abstract

Reaction between the dichloroboryl complex, Os(BCl$_2$)Cl(CO)(PPh$_3$)$_2$, and water replaces both chloride substituents on the boryl ligand, without cleavage of the Os–B bond, giving yellow Os[B(OH)$_2$]Cl(CO)(PPh$_3$)$_2$ (**1**). Compound **1** can be regarded as an example of a 'metalla–boronic acid' (L$_n$M–B(OH)$_2$) and in the solid state, X-ray crystal structure determination reveals that molecules of **1** are tetragonal pyramidal in geometry (Os–B, 2.056(3) Å) and are arranged in pairs, as hydrogen-bonded dimers. This same arrangement is found in the crystalline state for simple boronic acids. Reaction between the dichloroboryl complex, Os(BCl$_2$)Cl(CO)(PPh$_3$)$_2$, and methanol and ethanol produces yellow Os[B(OMe)$_2$]Cl(CO)(PPh$_3$)$_2$ (**2a**) and yellow Os[B(OEt)$_2$]Cl(CO)(PPh$_3$)$_2$ (**2b**), respectively. The crystal structure of **2b** reveals a tetragonal pyramidal geometry with the diethoxyboryl ligand in the apical site and with an Os–B bond distance of 2.081(5) Å. Reaction between Os(BCl$_2$)Cl(CO)(PPh$_3$)$_2$, and *N,N*′-dimethyl-*o*-phenylenediamine and *N,N*′-dimethyl-ethylenediamine produces yellow Os[BN(CH$_3$)C$_6$H$_4$N(CH$_3$)]Cl(CO)(PPh$_3$)$_2$ (**5**) and yellow Os[BN(CH$_3$)C$_2$H$_4$N(CH$_3$)]Cl(CO)(PPh$_3$)$_2$ (**6**), respectively. Compounds **1**, **2a**, **2b**, **5**, and **6** all react with carbon monoxide to give the colourless, six-coordinate complexes Os[B(OH)$_2$]Cl(CO)$_2$(PPh$_3$)$_2$ (**3**), Os[B(OMe)$_2$]Cl(CO)$_2$(PPh$_3$)$_2$ (**4a**), Os[B(OEt)$_2$]Cl(CO)$_2$(PPh$_3$)$_2$ (**4b**), Os[BN(CH$_3$)C$_6$H$_4$N(CH$_3$)]Cl(CO)$_2$(PPh$_3$)$_2$ (**7**), and Os[BN(CH$_3$)C$_2$H$_4$N(CH$_3$)]Cl(CO)$_2$(PPh$_3$)$_2$ (**8**), respectively, but in the case of **6** only, this CO uptake is easily reversible. The crystal structure of **5** is also reported.

1. Introduction

Compounds with transition metal–boron, 2c–2e bonds (L$_n$M–BR$_2$) have been widely studied in the past decade both because of their fundamental interest and their role as important intermediates in the metal-catalyzed syntheses of boron-functionalised organics. Several extensive reviews have covered developments in this area [1]. In organoboron chemistry, BCl$_3$ is of special significance because of the ease with which it is converted into a wide range of organoboron derivatives through facile substitution reactions of the chloride groups. In a similar way, L$_n$M–BCl$_2$, i.e. compounds

* Corresponding authors. Tel.: +64-9-373-7999 × 88320; fax: +64-9-373-7422.
E-mail address: w.roper@auckland.ac.nz (W.R. Roper).

containing the dichloroboryl ligand, offer the possibility of conversion to many interesting derivatives. We have previously described the conversion of $Os(BCl_2)Cl(CO)(PPh_3)_2$ to a complex containing a base-stabilised borylene ligand [2], and to the formation of tethered boryl and borylene complexes through reaction with either 2-hydroxypyridine [3] or 2-amino-pyridine [4]. Related substitution reactions of a metal-bridging B–Cl ligand have also been reported [5]. In this paper, we describe the very simple reactions of $Os(BCl_2)Cl(CO)(PPh_3)_2$ with water, alcohols and dia-mines. These reactions lead to: (i) the first dihydrox-yboryl complex, $Os[B(OH)_2]Cl(CO)(PPh_3)_2$; (ii) the dialkoxyboryl complexes, $Os[B(OR)_2]Cl(CO)(PPh_3)_2$; and (iii) the cyclic diaminoboryl complexes, $Os[BN(CH_3)C_6H_4N(CH_3)]Cl(CO)_2(PPh_3)_2$ and $Os[BN(CH_3)C_2H_4N(CH_3)]Cl(CO)_2(PPh_3)_2$. The further-reactions of these coordinatively unsaturated com-pounds with CO and crystal structures of examples of each of the above classes of compound are also reported.

2. Results and discussion

2.1. Reaction of $Os(BCl_2)Cl(CO)(PPh_3)_2$ with water and the structure of $Os[B(OH)_2]Cl(CO)(PPh_3)_2$ (1)

Treatment of $Os(BCl_2)Cl(CO)(PPh_3)_2$ with water in THF produces rapidly, the bright yellow dihydroxy-boryl complex, $Os[B(OH)_2]Cl(CO)(PPh_3)_2$ (1), in good yield (see Scheme 1). The $v(CO)$ for this compound is observed at 1917 cm^{-1}, lower than the position for
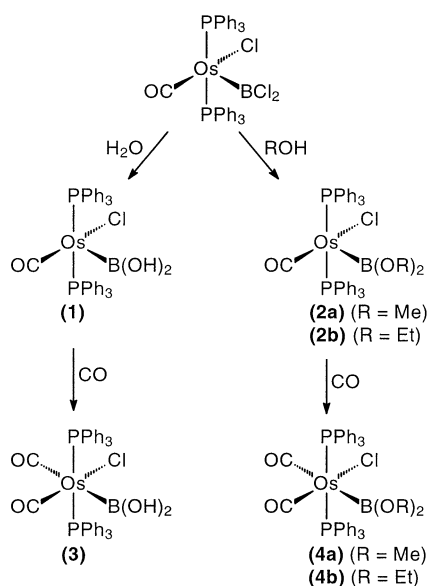
$v(CO)$ (1929 cm^{-1}) observed in $Os(BCl_2)Cl(CO)-(PPh_3)_2$. This is consistent with a decrease in the π-acceptor capacity of the $B(OH)_2$ ligand relative to BCl_2 as chloride is replaced by the better π-donating hydrox-ide group. The IR spectrum of 1 also reveals a broad band at 3301 cm^{-1} which is assigned to $v(OH)$. The broadness of this band suggests the presence of H-bonding and this is verified by the structure determina-tion described below. In the ^1H-NMR spectrum of 1, a broad resonance is observed at δ 4.46 ppm for the OH groups. This signal integrates for two protons and disappears on addition of D_2O.

The molecular geometry of 1 is shown in Fig. 1. Crystal data pertaining to this structure and other structures reported in this paper are presented in Table 1. Selected bond lengths and angles for 1 are collected in Table 2. The overall geometry about osmium is that of a tetragonal pyramid with the two triphenylphosphine ligands mutually trans and the boryl ligand occupying the apical site. The Os–B distance is 2.056(3) Å. This is longer than the Os–B distance found in the closely related complex, $Os(Bcat)Cl(CO)(PPh_3)_2$ (cat = 1,2-$O_2C_6H_4$) (2.019(3) Å) which has the same tetragonal pyramidal geometry [6]. This observation can be ratio-nalized in terms of a competitive π-donation situation where Os–B π-donation is relatively stronger in the Bcat complex, and O–B π-donation is relatively stronger in the $B(OH)_2$ complex. The angle between the CO and boryl ligands is 90.85(13)°.

An interesting feature revealed by the crystal structure of 1 is that molecules are grouped as pairs held together by two intermolecular H-bonds. The precise arrange-ment is depicted in Fig. 2, and this bears a very close resemblance to the pair-wise arrangement found in the crystal structure of phenylboronic acid [7]. The distance between O(1) and O(2′) (Fig. 2) is 2.768 Å. This lies in the middle of the range observed for O–H···O hydro-
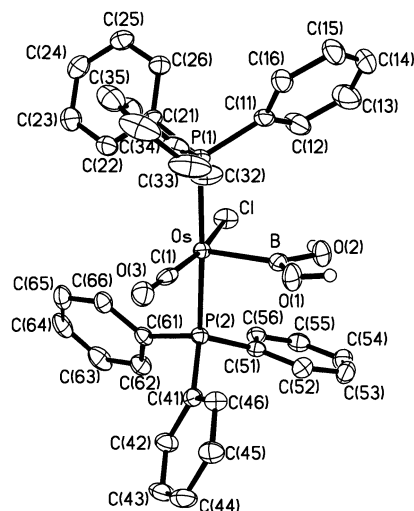

Scheme 1. Reactions of $Os(BCl_2)Cl(CO)(PPh_3)_2$ with water and alcohols.

Fig. 1. Molecular geometry of $Os[B(OH)_2]Cl(CO)(PPh_3)_2$ (1).

Table 1
Data collection and processing parameters [a]

Compound	1	2b	5
Empirical formula	$C_{37}H_{32}$- $BClO_3OsP_2$	$C_{41}H_{40}$- $BClO_3OsP_2$	$C_{45}H_{40}$- $BClN_2OOsP_2$
Molecular weight	823.03	879.13	923.19
Crystal system	triclinic	triclinic	orthorhombic
Space group	$P\bar{1}$	$P\bar{1}$	$P2_12_12_1$
a, (Å)	11.5505(2)	9.894(3)	11.450(2)
b, (Å)	11.8954(1)	11.992(5)	16.470(4)
c, (Å)	13.6687(1)	17.290(3)	20.366(17)
α, (°)	70.143(1)	77.05(2)	90.0
β, (°)	79.880(1)	88.41(2)	90.0
γ, (°)	73.515(1)	67.05(2)	90.0
V, (Å)^3	1687.21(3)	1836.9(10)	3841(3)
Z	2	2	4
D_{calc} (g cm^{-3})	1.620	1.589	1.597
$F(000)$	812	876	1840
μ (mm^{-1})	3.989	3.669	3.512
Crystal size (mm)	$0.12 \times 0.05 \times$ 0.05	$0.29 \times 0.11 \times$ 0.07	$0.50 \times 0.45 \times$ 0.40
θ (Min–max) (°)	1.85–27.08	1.90–25.03	1.59–29.97
Reflections collected	14 240	6821	6173
Independent reflections	7194, [R_{int} 0.020]	6485 [R_{int} 0.021]	6136 [R_{int} 0.063]
A (min–max)	0.6461, 0.8255	0.684, 0.997	0.3251, 0.4156
Goodness-of-fit on F^2	1.034	0.771	0.932
R, wR_2 (observed data)	0.0226, 0.0499	0.0281, 0.0710	0.0459, 0.1269
R, wR_2 (all data)	0.0265, 0.0515	0.0372, 0.0764	0.0634, 0.1385

[a] $R = \Sigma||F_o|-|F_c||/\Sigma|F_o|$. $wR_2 = \{\Sigma[w(F_o^2 - F_c^2)^2]/\Sigma[w(F_o^2)^2]\}^{\frac{1}{2}}$.

Table 2
Selected bond lengths [Å] and angles [°] for 1

Bond lengths	
Os–C(1)	1.844(3)
Os–B	2.056(3)
Os–P(2)	2.3677(7)
Os–P(1)	2.3720(7)
Os–Cl	2.4210(8)
O(1)–B	1.361(4)
O(1)–H(1)	0.89(5)
O(2)–B	1.397(4)
O(2)–H(2)	0.76(5)
O(3)–C(1)	1.130(4)
Bond angles	
C(1)–Os–B	90.85(13)
C(1)–Os–P(2)	91.04(8)
B–Os–P(2)	93.70(9)
C(1)–Os–P(1)	91.91(8)
B–Os–P(1)	90.55(9)
P(2)–Os–P(1)	174.79(2)
C(1)–Os–Cl	168.17(8)
B–Os–Cl	100.91(10)
P(2)–Os–Cl	86.97(3)
P(1)–Os–Cl	89.28(3)
B–O(1)–H(1)	107(3)
B–O(2)–H(2)	115(4)
O(3)–C(1)–Os	177.2(2)
O(1)–B–O(2)	116.1(3)
O(1)–B–Os	126.9(2)
O(2)–B–Os	116.9(2)

gen bonding (2.48–2.90 Å) [8]. In addition, in each molecule there may be a weak intramolecular hydrogen bond between one OH group and the adjacent chloride bound to osmium. The distance between O(2) and Cl (3.348 Å) is, however, long.

2.2. Reaction of Os(BCl₂)Cl(CO)(PPh₃)₂ with alcohols and the structure of Os[B(OEt)₂]Cl(CO)(PPh₃)₂ (2b)

Treatment of Os(BCl₂)Cl(CO)(PPh₃)₂ with methanol or ethanol in THF produces the bright yellow dimethoxyboryl complex, Os[B(OMe)₂]Cl(CO)(PPh₃)₂ (2a), or the bright yellow diethoxyboryl complex, Os[B(OEt)₂]Cl(CO)(PPh₃)₂ (2b), respectively, in good yield (see Scheme 1). Both complexes show no tendency to undergo transesterification reactions when recrystallised in the presence of other alcohols. Furthermore, in contrast to methyl or ethyl borate, (B(OR)₃), 2a and 2b did not readily undergo hydrolysis even when recrystallised from wet solvents. In the IR spectra of 2a and 2b, the *v*(CO) bands are observed at 1908 and 1906 cm^{-1}, respectively. These values are lower than that observed for 1 (1917 cm^{-1}), suggesting that,
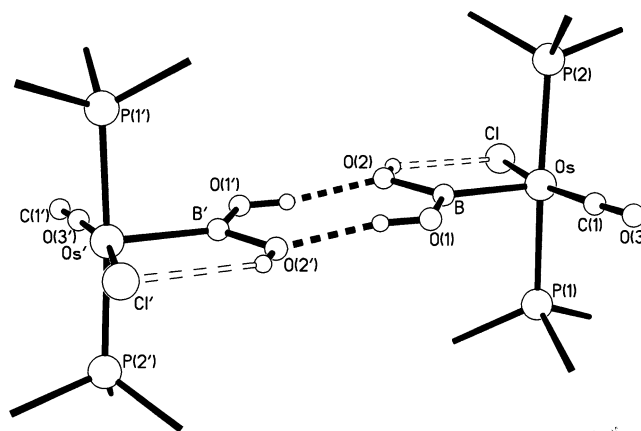

Fig. 2. Hydrogen-bond interactions between pairs of Os[B(OH)₂]Cl(CO)(PPh₃)₂ molecules in the crystalline state.

overall, B(OR)₂ ligands are more electron-releasing towards osmium than the B(OH)₂ ligand.

The molecular geometry of 2b is shown in Fig. 3. Selected bond lengths and angles for 2b are collected in Table 3. The overall geometry about osmium is the same as that observed for 1. The Os–B distance is 2.081(5) Å. This is slightly longer than the Os–B distance found in 1 (2.056(3) Å). The two B–O distances are 1.366(7) and 1.375(7) Å. These can be compared with the two B–O distances found in Os(Bcat)Cl(CO)(PPh₃)₂ which were
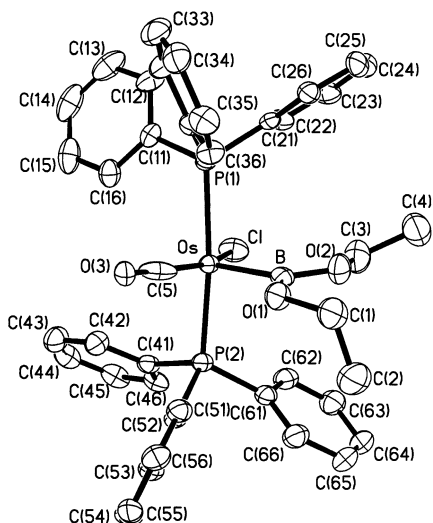
Fig. 3. Molecular geometry of Os[B(OEt)$_2$]Cl(CO)(PPh$_3$)$_2$ (**2b**).

1.411(4) and 1.406(4) Å. Clearly, shorter Os−B distances are associated with longer B−O distances in related examples, an observation compatible with a competitive π-bonding model.
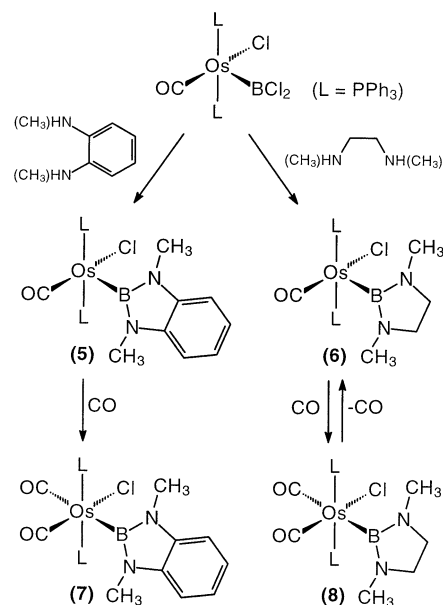
2.3. Reaction of Os(BCl$_2$)Cl(CO)(PPh$_3$)$_2$ with amines and the structure of Os[BN(CH$_3$)C$_6$H$_4$N(CH$_3$)]Cl(CO) (PPh$_3$)$_2$ (5)

In contrast to the straightforward reactions observed between Os(BCl$_2$)Cl(CO)(PPh$_3$)$_2$ and alcohols, preliminary experiments involving treatment of Os(BCl$_2$)-Cl(CO)(PPh$_3$)$_2$ with either dimethylamine or *p*-toluidine did not lead to products retaining an Os−B bond. Attention was therefore directed towards suitable diamines where there was the possibility for the formation of cyclic diaminoboryl ligands, which might confer greater stability on the resulting complexes. Accordingly, reactions of Os(BCl$_2$)Cl(CO)(PPh$_3$)$_2$ with N,N′-dimethyl-*o*-phenylenediamine and N,N′-dimethyl-ethylenediamine were investigated. As depicted in Scheme 2, these reactions led to yellow Os[BN(CH$_3$)C$_6$H$_4$N(CH$_3$)]-Cl(CO)(PPh$_3$)$_2$ (**5**) and yellow Os[BN(CH$_3$)C$_2$H$_4$N-(CH$_3$)]Cl(CO)(PPh$_3$)$_2$ (**6**), respectively. Unlike the O-substituted boryl complexes **1**, **2a**, and **2b** described above the N-substituted complexes **5** and **6** cannot be handled, in solution, in the presence of water or alcohols. The compounds decompose to give uncharacterised products which contain Os−H bonds but do not contain Os−B bonds. Complex **5** is much more stable than complex **6**. In the IR spectrum of **5**, there is a band assigned to ν(CO) at 1885 cm^{-1}. The corresponding band for **6** is at 1890 cm^{-1}. Both these bands are lower than those observed for the O-substituted com-

Table 3
Selected bond lengths [Å] and angles [°] for **2b**

Bond lengths	
Os−C(5)	1.861(7)
Os−B	2.081(5)
Os−P(1)	2.3660(14)
Os−P(2)	2.3673(14)
Os−Cl	2.3974(15)
B−O(2)	1.366(7)
B−O(1)	1.375(7)
O(1)−C(1)	1.433(6)
O(2)−C(3)	1.411(7)
O(3)−C(5)	1.034(7)
C(1)−C(2)	1.490(9)
C(3)−C(4)	1.513(9)
Bond angles	
C(5)−Os−B	89.6(2)
C(5)−Os−P(1)	89.90(15)
B−Os−P(1)	96.34(14)
C(5)−Os−P(2)	93.45(15)
B−Os−P(2)	93.02(14)
P(1)−Os−P(2)	170.07(4)
C(5)−Os−Cl	156.92(18)
B−Os−Cl	113.48(17)
P(1)−Os−Cl	86.88(5)
P(2)−Os−Cl	86.38(5)
O(2)−B−O(1)	113.5(4)
O(2)−B−Os	125.0(4)
O(1)−B−Os	121.5(4)
B−O(1)−C(1)	121.8(4)
B−O(2)−C(3)	128.2(4)

plexes suggesting that N-substituted boryl ligands are better overall electron donors. In the ^{1}H-NMR spectra of **5** and **6**, the *N*-methyl groups are inequivalent and give rise to two signals in each case, at 2.41 and 2.42 ppm for **5**, and at 1.82 and 1.85 ppm for **6**. This indicates

Scheme 2. Reactions of Os(BCl$_2$)Cl(CO)(PPh$_3$)$_2$ with amines.
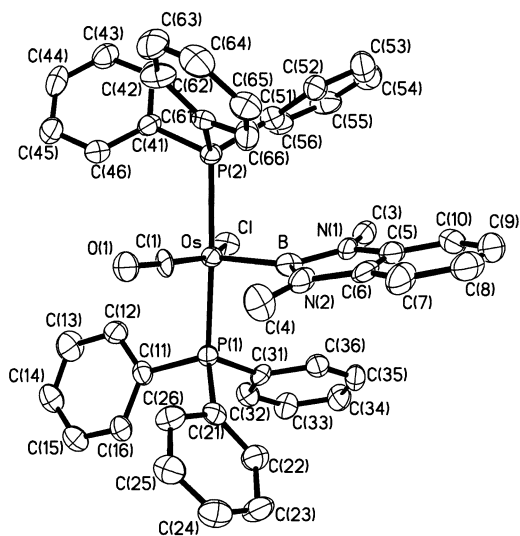
Fig. 4. Molecular geometry of Os[BN(CH$_3$)C$_6$H$_4$N(CH$_3$)]Cl(CO)-(PPh$_3$)$_2$ (**5**).

Table 4
Selected bond lengths [Å] and angles [°] for **5**

Bond lengths	
Os–C(1)	1.711(13)
Os–B	2.082(10)
Os–P(1)	2.365(2)
Os–P(2)	2.371(2)
Os–Cl	2.437(4)
B–N(2)	1.436(13)
B–N(1)	1.491(15)
N(1)–C(5)	1.405(13)
N(1)–C(3)	1.421(15)
N(2)–C(6)	1.394(14)
N(2)–C(4)	1.471(15)
Bond angles	
C(1)–Os–B	94.2(6)
C(1)–Os–P(1)	93.5(5)
B–Os–P(1)	93.6(3)
C(1)–Os–P(2)	89.7(5)
B–Os–P(2)	91.8(3)
P(1)–Os–P(2)	173.53(8)
C(1)–Os–Cl	151.0(6)
B–Os–Cl	114.8(4)
P(1)–Os–Cl	85.96(11)
P(2)–Os–Cl	88.51(11)
O(1)–C(1)–Os	173.6(15)
N(2)–B–N(1)	104.0(8)
N(2)–B–Os	131.7(9)
N(1)–B–Os	124.0(7)

that rotation about the Os–B bond is slow on the NMR timescale at 25 °C, probably as a result of steric interactions between the methyl groups and the bulky, mutually *trans* triphenylphosphine ligands.

The molecular geometry of **5** is shown in Fig. 4. Selected bond lengths and angles for **5** are collected in Table 4. The overall geometry about osmium is again the same as that observed for **1**. In the crystal structure of **5**, the CO and Cl ligands are disordered. The Os–B distance is 2.082(10) Å. This is almost exactly the same as the Os–B distance found in **2b** (2.081(5) Å). The two B–N distances are 1.436(13) and 1.491(15) Å. These are long as can be seen from a comparison with the mean for all previously determined B–N distances (1.424, SD 0.043 Å) [9]. The *o*-phenylene group bridging between the two N atoms must reduce the electron donor capacity of the N atoms towards the B atom.

2.4. Reactions of the five-coordinate boryl complexes with carbon monoxide

The coordinatively unsaturated dichloroboryl complex, Os(BCl$_2$)Cl(CO)(PPh$_3$)$_2$, takes up CO readily but the product isolated, regardless of all our efforts to exclude moisture, was the hydrolysis product, the dihydroxyboryl complex, Os[B(OH)$_2$]Cl(CO)$_2$(PPh$_3$)$_2$ (**3**). This implies that the reactivity of the dichloroboryl ligand is greatly increased in the coordinatively saturated complex where it is located trans to a π-accepting CO ligand. Complex **3** can also be prepared by direct addition of CO to complex **1**. The first route is the highest yielding, and is the one described in the Section 4. Similarly, the complexes, **2a**, **2b**, and **5** all add CO irreversibly to give the dicarbonyl complexes, Os[B(O-Me)$_2$]Cl(CO)$_2$(PPh$_3$)$_2$ (**4a**), Os[B(OEt)$_2$]Cl(CO)$_2$(PPh$_3$)$_2$ (**4b**), and Os[BN(CH$_3$)C$_6$H$_4$N(CH$_3$)]Cl(CO)$_2$(PPh$_3$)$_2$ (**7**), respectively. In the IR spectra, all of these compounds display two ν(CO) bands at very similar positions, e.g. for **3** these bands are at 2012 and 1944 cm^{-1}, indicating that the two CO ligands are located in mutually cis positions. The behaviour of complex, Os[BN(CH$_3$)C$_2$H$_4$N(CH$_3$)]Cl(CO)(PPh$_3$)$_2$ (**6**), is anomalous, in that CO uptake is readily reversible. Solutions of the yellow complex **6** become colourless under CO pressure but the solid isolated from solution was always composed of a mixture of **6** (ν(CO): 1890 cm^{-1}) and **8** (ν(CO): 2020, 1929 cm^{-1}).

3. Conclusions

The coordinatively unsaturated dichloroboryl complex, Os(BCl$_2$)Cl(CO)(PPh$_3$)$_2$, is an excellent synthon for oxygen-substituted boryl complexes and reaction with water and with simple alcohols occurs readily to give the dihydroxyboryl complex, Os[B(OH)$_2$]Cl-(CO)(PPh$_3$)$_2$ (**1**), and the dialkoxyboryl complexes, Os[B(OR)$_2$]Cl(CO)(PPh$_3$)$_2$ (**2a**, **2b**), respectively, in good yield. Crystal structure determinations of complexes **1**, **2b**, and **5** reveal a tetragonal pyramidal geometry about osmium with the group with the largest trans influence, the boryl ligand, apical. In the solid

state, the molecules of **1** occur as H-bonded pairs. In contrast to the reactions with oxygen nucleophiles, reaction between $Os(BCl_2)Cl(CO)(PPh_3)_2$ and simple amines leads to rupture of the Os–B bond and isolated aminoboryl complexes are restricted to examples with cyclic diaminoboryl ligands derived from reaction with *N,N'*-dimethyl-*o*-phenylenediamine and *N,N'*-dimethyl-ethylenediamine. All of these coordinatively unsaturated boryl complexes react with CO to give the corresponding six coordinate dicarbonyl complexes. However, in one case, complex **6**, the addition is reversible, suggesting that a diaminoboryl ligand can have a very pronounced trans influence, clearly even greater than the trans influence exhibited by dialkoxyboryl ligands.

4. Experimental

4.1. General procedures and instruments

Standard laboratory procedures were followed as have been described previously [10]. The compound $Os(BCl_2)Cl(CO)(PPh_3)_2$ [11] was prepared according to the literature method.

Infrared spectra (4000–400 cm^{-1}) were recorded as Nujol mulls between KBr plates on a Perkin–Elmer Paragon 1000 spectrometer. NMR spectra were obtained on a Bruker DRX 400 at 25 °C. ^{1}H-, ^{13}C-, ^{11}B-, and ^{31}P-NMR spectra were obtained operating at 400.1 (^{1}H), 100.6 (^{13}C), 128.0 (^{11}B), and 162.0 (^{31}P) MHz, respectively. Resonances are quoted in ppm and ^{1}H-NMR spectra referenced to either tetramethylsilane (0.00 ppm) or the proteo-impurity in the solvent (7.25 ppm for CHCl$_3$). ^{13}C-NMR spectra were referenced to CDCl$_3$ (77.00 ppm), ^{11}B-NMR spectra to BF$_3$·OEt$_2$ as an external standard (0.00 ppm), and ^{31}P-NMR spectra to 85% orthophosphoric acid (0.00 ppm) as an external standard. Elemental analyses were obtained from the Microanalytical Laboratory, University of Otago.

4.2. Preparation of $Os[B(OH)_2]Cl(CO)(PPh_3)_2$ (**1**)

$Os(BCl_2)Cl(CO)(PPh_3)_2$ (0.160 g, 0.186 mmol) was dissolved in THF (7 mL) to which had been added one drop of H$_2$O. The yellow solution was stirred for 30 s and then the solvent volume was reduced in vacuo to ca. 2 mL. Slow addition of *n*-hexane effected the crystallisation of the yellow product **1**. This product was of high purity and suitable for most purposes. However, for microanalysis, it was recrystallised from the ternary solvent system, CH$_2$Cl$_2$–C$_2$H$_5$OH–*n*-hexane (0.110 g, 72%). Anal. Calc. for C$_{37}$H$_{32}$BClO$_3$OsP$_2$: C, 53.99; H, 3.92. Found C, 54.10; H, 3.60%. IR (cm^{-1}): 1917 ν(CO); 3301 ν(OH); 1348, 1312, 1240, 1192, 1026. ^{1}H-NMR (C$_6$D$_6$; δ): 4.46 (s broad, 2H, B(O*H*)$_2$), 6.96–7.10 and 7.82–7.87 (m, 30H, PPh$_3$).

4.3. Preparation of $Os[B(OMe)_2]Cl(CO)(PPh_3)_2$ (**2a**)

$Os(BCl_2)Cl(CO)(PPh_3)_2$ (0.130 g, 0.151 mmol) was dissolved in a mixture of THF (10 mL) and CH$_3$OH (2 mL). The resulting yellow solution was stirred for ca. 5 min. Reduction of solvent volume in vacuo followed by slow addition of *n*-hexane afforded a bright yellow precipitate. Recrystallisation from CH$_2$Cl$_2$–C$_2$H$_5$OH gave bright yellow microcrystals of **2a** (0.086 g, 67%). Anal. Calc. for C$_{39}$H$_{36}$BClO$_3$OsP$_2$: C, 55.04; H, 4.26. Found C, 54.92; H, 4.01%. IR (cm^{-1}): 1908 ν(CO); 1269, 1244, 1215, 1159, 1122, 1001, 610. ^{1}H-NMR (C$_6$D$_6$; δ): 3.45 (s, 6H, OC*H*$_3$), 6.89–7.15 and 7.84–8.02 (m, 30H, PPh$_3$).

4.4. Preparation of $Os[B(OEt)_2]Cl(CO)(PPh_3)_2$ (**2b**)

$Os(BCl_2)Cl(CO)(PPh_3)_2$ (0.150 g, 0.174 mmol) was dissolved in a mixture of THF (10 mL) and C$_2$H$_5$OH (2 mL) and treated as in Section 4.3 above. Recrystallisation from CH$_2$Cl$_2$–C$_2$H$_5$OH gave bright yellow microcrystals of **2b** (0.121 g, 79%). Anal. Calc. for C$_{41}$H$_{40}$BClO$_3$OsP$_2$: C, 56.01; H, 4.59. Found C, 55.61; H, 4.20%. IR (cm^{-1}): 1906 ν(CO); 1246, 1221, 1190, 1179, 1126, 1037, 893. ^{1}H-NMR (CDCl$_3$; δ): 0.82 (t, 6H, OCH$_2$C*H*$_3$, $^{3}J_{HH}$ = 7.0 Hz); 3.45 (q, 4H, OC*H*$_2$CH$_3$, $^{3}J_{HH}$ = 7.0 Hz); 7.32–7.40 and 7.60–7.67 (m, 30H, PPh$_3$). ^{13}C-NMR (CDCl$_3$; δ): 17.1 (s, OCH$_2$*C*H$_3$); 60.1 (s, O*C*H$_2$CH$_3$); 128.0 (t' [10], PPh$_3$ *ortho*, $^{2,4}J_{CP}$ = 9.9 Hz); 130.0 (s, PPh$_3$ *para*); 133.2 (t', PPh$_3$ *ipso*, $^{1,3}J_{CP}$ = 49.5 Hz); 134.6 (t', PPh$_3$ *meta*, $^{3,5}J_{CP}$ = 11.4 Hz); 184.2 (t, *C*O, $^{2}J_{CP}$ = 9.6 Hz).

4.5. Preparation of $Os[B(OH)_2]Cl(CO)_2(PPh_3)_2$ (**3**)

$Os(BCl_2)Cl(CO)(PPh_3)_2$ (0.820 g, 0.953 mmol) was dissolved in wet THF (10 mL) in a Fisher–Porter bottle and pressurised with carbon monoxide (4 atm). The initially yellow solution rapidly changed to a pale orange on admission of CO, stirring was continued for 30 s. The pressure was then released and H$_2$O (1 mL) was added. The solution was re-pressurised with CO and stirred for a further 30 s. Addition of C$_2$H$_5$OH followed by slow evaporation of the solvent on a rotary evaporator precipitated an almost colourless product. Recrystallisation from CH$_2$Cl$_2$–C$_2$H$_5$OH gave colourless microcrystals of **3** (0.580 g, 71%). Anal. Calc. for C$_{38}$H$_{32}$BClO$_4$OsP$_2$: C, 53.63; H, 3.79. Found C, 53.55; H, 3.59%. IR (cm^{-1}): 2012, 1944 ν(CO); 3470, 3364 ν(OH); 1377, 1296, 1242, 1049, 1011. ^{1}H-NMR (CDCl$_3$; δ): 5.04 (s, 2H, B(O*H*)$_2$); 6.96–7.10 and 7.82–7.87 (m,

30H, PPh$_3$). ^{11}B-NMR (CDCl$_3$; δ): 43.7 (s broad). ^{31}P-NMR (CDCl$_3$; δ): −2.0 (s).

4.6. Preparation of Os[B(OMe)$_2$]Cl(CO)$_2$(PPh$_3$)$_2$ (4a)

Compound 2a (0.100 g, 0.117 mmol) was dissolved in THF (10 mL) in a Fisher–Porter bottle and pressurised with carbon monoxide (4 atm) while stirring at room temperature (r.t.). The yellow solution rapidly decolourised on pressurisation with CO. Stirring was continued for a further 5 min. Addition of C$_2$H$_5$OH followed by slow evaporation of solvent on a rotary evaporator effected crystallisation of a colourless product. Recrystallisation from CH$_2$Cl$_2$–C$_2$H$_5$OH gave colourless microcrystals of 4a (0.088 g, 85%). Anal. Calc. for C$_{40}$H$_{36}$BClO$_4$OsP$_2$: C, 54.65; H, 4.13. Found C, 54.88; H, 3.99%. IR (cm^{-1}): 2016, 1940 ν(CO); 1255, 1215, 1190, 1155, 1123, 1003. ^{1}H-NMR (CDCl$_3$; δ): 3.06 (s, 6H, OCH$_3$); 7.33–7.39 and 7.60–7.72 (m, 30H, PPh$_3$). ^{13}C-NMR (CDCl$_3$; δ): 52.2 (s, OCH$_3$); 127.8 (t′ [10], PPh$_3$ ortho, $^{2,4}J_{CP}$ = 10.2 Hz); 130.1 (s, PPh$_3$ para); 134.0 (t′, PPh$_3$ ipso, $^{1,3}J_{CP}$ = 52.3 Hz); 134.1 (t′, PPh$_3$ meta, $^{3,5}J_{CP}$ = 10.7 Hz); 181.1 (t, CO, $^2J_{CP}$ = 8.0 Hz); 183.4 (t, CO, $^2J_{CP}$ = 8.4 Hz). ^{31}P-NMR (CDCl$_3$; δ): −3.6 (s).

4.7. Preparation of Os[B(OEt)$_2$]Cl(CO)$_2$(PPh$_3$)$_2$ (4b)

Compound 2b (0.150 g, 0.171 mmol) was dissolved in THF (10 mL) in a Fisher–Porter bottle and treated as in Section 4.6 above. Recrystallisation from CH$_2$Cl$_2$–C$_2$H$_5$OH gave colourless microcrystals of 4b (0.111 g, 72%). Anal. Calc. for C$_{42}$H$_{40}$BClO$_4$OsP$_2$: C, 55.61; H, 4.44. Found C, 55.16; H, 4.21%. IR (cm^{-1}): 2020, 1939 ν(CO); 1306, 1259, 1219, 1192, 1171, 1159, 1038. ^{1}H-NMR (CDCl$_3$; δ): 0.78 (t, 6H, OCH$_2$CH$_3$, $^3J_{HH}$ = 7.0 Hz); 3.44 (q, 4H, OCH$_2$CH$_3$, $^3J_{HH}$ = 7.0 Hz); 7.32–7.40 and 7.60–7.72 (m, 30H, PPh$_3$).

4.8. Preparation of Os[B̅N(CH$_3$)C$_6$H$_4$N̅(CH$_3$)]Cl(CO)(PPh$_3$)$_2$ (5)

Os(BCl$_2$)Cl(CO)(PPh$_3$)$_2$ (0.200 g, 0.233 mmol) was dissolved in C$_6$H$_6$ (20 mL). N,N′-dimethyl-o-phenylenediamine (0.063 g, 0.47 mmol) was then added to the rapidly stirred solution. On addition, the initially yellow-orange solution intensified to an intense orange colour over the course of 1–2 min. During this time, a small amount of colourless amine hydrochloride salt of the aromatic diamine was precipitated. Following filtration, the resulting solution was reduced in volume in vacuo then n-hexane was added to effect crystallisation of orange microcrystals. The product was washed with a small portion of cold C$_2$H$_5$OH and recrystallised from

C$_6$H$_6$–n-hexane to afford orange microcrystals of 5 (0.137 g, 64%). Anal. Calc. for C$_{45}$H$_{40}$BClN$_2$OOsP$_2$: C, 58.54; H, 4.37; N, 3.03. Found C, 58.31; H, 4.43; N, 2.79%. IR (cm^{-1}): 1885 ν(CO); 1335, 1306, 1270, 1216, 1050, 1026. ^{1}H-NMR (CDCl$_3$; δ): 2.41 (s, 3H, NCH$_3$); 2.42 (s, 3H, NCH$_3$); 6.60–6.74 (m, 2H, C$_6$H$_4$); 6.81–6.88 (m, 2H, C$_6$H$_4$); 7.23–7.53 (m, 30H, PPh$_3$). ^{13}C-NMR (C$_6$D$_6$; δ): 30.5 (s, NCH$_3$); 32.1 (s, NCH$_3$); 106.5 (s, C$_6$H$_4$); 106.6 (s, C$_6$H$_4$); 118.1 (s, C$_6$H$_4$); 118.3 (s, C$_6$H$_4$); 128.4 (t′ [10], PPh$_3$ ortho, $^{2,4}J_{CP}$ = 10.1 Hz); 130.2 (s, PPh$_3$ para); 133.9 (t′, PPh$_3$ ipso, $^{1,3}J_{CP}$ = 50.3 Hz); 135.0 (t′, PPh$_3$ meta, $^{3,5}J_{CP}$ = 11.1 Hz); 140.1 (s, C$_6$H$_4$, quaternary); 141.0 (s, C$_6$H$_4$, quaternary); 186.8 (t, CO, $^2J_{CP}$ = 9.1 Hz).

4.9. Preparation of Os[B̅N(CH$_3$)C$_2$H$_4$N̅(CH$_3$)]Cl(CO)(PPh$_3$)$_2$ (6)

Os(BCl$_2$)Cl(CO)(PPh$_3$)$_2$ (0.500 g, 0.581 mmol) was dissolved in C$_6$H$_6$ (30 mL). N,N′-dimethyl-ethylenediamine (1.238 mL, 11.63 mmol) was then added and the solution was stirred rapidly for 30 min at r.t. During this time, the solution became more orange in colour and an amount of colourless amine hydrochloride salt of the diamine was precipitated. Following filtration, the resulting solution was reduced in volume in vacuo to ca. 1.5 mL and then n-hexane was added to effect crystallisation of a vibrant yellow microcrystalline precipitate. Recrystallisation from C$_6$H$_6$–n-hexane gave bright yellow microcrystals of 6 (0.417 g, 82%). ^{1}H-NMR indicates the presence of 1.0 equivalent of water of crystallisation. Anal. Calc. for C$_{41}$H$_{40}$BClN$_2$OOsP$_2$·H$_2$O: C, 55.13; H, 4.74; N, 3.14. Found C, 55.15; H, 4.84; N, 3.23%. IR (cm^{-1}): 1890 ν(CO); 1273, 1231, 1188, 1059, 988. ^{1}H-NMR (CDCl$_3$; δ): 1.82 (s, 3H, NCH$_3$); 1.85 (s, 3H, NCH$_3$); 3.03 (m, 4H, C$_2$H$_4$); 7.27–7.40 and 7.57–7.64 (m, 30H, PPh$_3$). ^{13}C-NMR (CDCl$_3$; δ): 35.2 (s, NCH$_3$); 36.9 (s, NCH$_3$); 52.9 (s, C$_2$H$_4$); 53.9 (s, C$_2$H$_4$); 127.9 (t′ [10], PPh$_3$ ortho, $^{2,4}J_{CP}$ = 9.1 Hz); 129.8 (s, PPh$_3$ para); 133.7 (t′, PPh$_3$ ipso, $^{1,3}J_{CP}$ = 39.2 Hz); 134.7 (t′, PPh$_3$ meta, $^{3,5}J_{CP}$ = 11.1 Hz); 186.3 (t, CO, $^2J_{CP}$ = 9.6 Hz).

4.10. Preparation of Os[B̅N(CH$_3$)C$_6$H$_4$N̅(CH$_3$)]Cl(CO)$_2$(PPh$_3$)$_2$ (7)

Compound 5 (0.090 g, 0.097 mmol) was dissolved in C$_6$H$_6$ (15 mL) in a Fisher–Porter bottle and pressurised with carbon monoxide (4 atm) while stirring at r.t. The orange solution decolourised rapidly on pressurisation with CO. Stirring was continued for a further 15 min. Addition of equal portions of C$_2$H$_5$OH–n-hexane followed by slow solvent evaporation on a rotary evaporator effected crystallisation of a nearly colourless product. Recrystallisation from CH$_2$Cl$_2$–C$_2$H$_5$OH–n-hexane gave colourless microcrystals of 7 (0.070 g, 75%).

Anal. Calc. for $C_{46}H_{40}BClN_2O_2OsP_2$: C, 58.08; H, 4.24; N, 2.94. Found C, 58.22; H, 4.86; N, 2.57%. IR (cm^{-1}): 2021, 1933 ν(CO); 1333, 1310, 1273, 1215, 1190, 1018, 623, 615. ^{1}H-NMR (CDCl$_3$; δ): 2.39 (s, 3H, NCH_3); 2.50 (s, 3H, NCH_3); 7.12–7.25 (m, 2H, C_6H_4); 7.36–7.42 (m, 2H, C_6H_4); 7.15–7.45 (m, 30H, PPh$_3$).

4.11. X-ray crystal structure determinations for complexes 1, 2b, and 5

Data were collected for **1** on a Siemens SMART CCD diffractometer at 150 K with graphite-monochromated Mo–K$_a$ radiation (λ 0.71073 Å) using ω scans. The data were corrected for Lorentz and polarization effects and absorption corrections applied using symmetry-related measurements [12]. For **2b** and **5**, data were collected on an Enraf-Nonius CAD4 diffractometer at 193 and 150 K, respectively, with graphite-monochromated Mo–K$_a$ radiation (λ 0.71073 Å) using $\omega/2\theta$ scans. Absorption corrections were applied using empirical ψ scan data [13]. Structures were solved using SHELXS [14] and refined by full-matrix least-squares using SHELXL [15] with anisotropic thermal parameters for all non-hydrogen atoms. Hydrogen atoms for **1** were located in a difference map and individually refined with isotropic temperature factors; for **2b** and **5** hydrogen atoms were included in calculated positions and allowed to ride on the carrier atom. In the crystal structure of **5**, the coordinated Cl and CO groups are disordered, and they were refined with partial occupancies summing to 1.0. Data in Table 4 and the atom positions in Fig. 4 are for the model with the larger occupancy (0.647). Crystal data and refinement details for all three structures are given in Table 1.

5. Supplementary material

Crystallographic data (excluding structure factors) have been deposited with the Cambridge Crystallographic Data Centre as supplementary publication nos. 200836–200838 for compounds **1**, **2b**, and **5**. Copies of this information can be obtained free of charge from The Director, CCDC, 12 Union Road, Cambridge, CB2 1EZ, UK (Fax: +44-1223-336033; e-mail: deposit@ccdc.cam.ac.uk or www: http://www.ccdc.cam.ac.uk).

References

[1] (a) H. Wadepohl, Angew. Chem. Int. Ed. Engl. 36 (1997) 2441;
(b) H. Braunschweig, Angew. Chem. Int. Ed. Engl. 37 (1998) 1786;
(c) G.J. Irvine, M.J.G. Lesley, T.B. Marder, N.C. Norman, C.R. Rice, E.G. Robins, W.R. Roper, G.R. Whittell, L.J. Wright, Chem. Rev. 98 (1998) 2685;
(d) T.B. Marder, N.C. Norman, in: W. Leitner, D.G. Blackmond (Eds.), Topics in Catalysis, vol. 5, Baltzer Science Publishers, Amsterdam, 1998, p. 63;
(e) M.R. Smith, III, Prog. Inorg. Chem. 48 (1999) 505;
(f) H. Braunschweig, M. Colling, Coord. Chem. Rev. 223 (2001) 1.
[2] G.J. Irvine, C.E.F. Rickard, W.R. Roper, A. Williamson, L.J. Wright, Angew. Chem. Int. Ed. 39 (2000) 948.
[3] C.E.F. Rickard, W.R. Roper, A. Williamson, L.J. Wright, Organometallics 21 (2002) 1714.
[4] C.E.F. Rickard, W.R. Roper, A. Williamson, L.J. Wright, Organometallics 21 (2002) 4862.
[5] H. Braunschweig, M. Müller, Chem. Ber./Recueil 130 (1997) 1295.
[6] C.E.F. Rickard, W.R. Roper, A. Williamson, L.J. Wright, Organometallics 17 (1998) 4869.
[7] S.J. Rettig, J. Trotter, Can. J. Chem. 55 (1977) 3071.
[8] A. Earnshaw, N.N. Greenwood, Chemistry of the Elements, Pergamon Press, New York, 1984, p. 6.
[9] Cambridge Crystallographic Data Base.
[10] S.M. Maddock, C.E.F. Rickard, W.R. Roper, L.J. Wright, Organometallics 15 (1996) 1793.
[11] G.J. Irvine, C.E.F. Rickard, W.R. Roper, A. Williamson, L.J. Wright, Angew. Chem. Int. Ed. 39 (2000) 948.
[12] R.H. Blessing, Acta Crystallogr. A51 (1995) 33.
[13] A.C.T. North, D.C. Phillips, F.S. Matthews, Acta Crystallogr. A24 (1968) 351.
[14] G.M. Sheldrick, Acta Crystallogr. A46 (1990) 467.
[15] G.M. Sheldrick, SHELXL, Program for Refinement of Crystal Structures, University of Göttingen, Göttingen, Germany, 1997.